

<https://doi.org/10.1038/s41531-025-00988-z>

Genetic risk and plasma biomarkers of dementia with Lewy bodies in a Chinese population

Check for updates

Xiaoli Hao¹, Xuwen Xiao^{1,2,3,4,5}, Ling Weng^{1,2,3,4,5}, Zhuojie Lin¹, Qian Xu^{1,2,3,4,5}, Juan Du^{1,2,3,4,5}, Qijie Yang¹, Yuan Zhu¹, Yiliang Liu¹, Tianyan Xu¹, Yafang Zhou⁶, Xinxin Liao⁶, Jifeng Guo^{1,2,3,4,5}, Shilin Luo^{1,2,3,4,5}, Junling Wang^{1,2,3,4,5}, Xinxiang Yan^{1,2,3,4,5}, Beisha Tang^{1,2,3,4,5,7,8}, Jinchen Li², Bin Jiao^{1,2,3,4,5} ✉ & Lu Shen^{1,2,3,4,5,7,8} ✉

Genetic investigations and associations with plasma biomarkers of dementia with Lewy bodies (DLB) in East Asian populations are lacking. The aim of our study is to identify candidate pathogenic variants and assess the diagnostic performance of plasma biomarkers among DLB patients in the Chinese population. This cohort included 151 DLB patients and 2010 controls, all of whom underwent whole genome sequencing. Plasma glial fibrillary acidic protein (GFAP), α -synuclein (α Syn), neurofilament light (NfL), and phosphorylated tau 217 (p-tau217) were detected in a subgroup. As a result, the *APOE* ϵ 4 allele significantly increased DLB risk ($p = 1.84E-11$), while rare missense variants of *USP13* gene were first found to be suggestively associated with DLB risk ($p = 1.31E-5$). Higher levels of plasma GFAP, α Syn, NfL, and p-tau217 were detected in DLB patients compared to controls ($p < 0.001$), which combined with polygenic risk scores (PRS) achieving an AUC of 0.927 for DLB diagnosis. Besides, significant correlations were observed between PRS of DLB and age at onset, the cumulative incidence rate, as well as plasma GFAP levels. In conclusion, this is the first study to simultaneously investigate the genetics and plasma biomarkers of DLB, highlighting the discriminative ability for DLB using PRS and plasma biomarker assay.

Dementia with Lewy bodies (DLB) is the second most common neurodegenerative dementia, with core clinical features of fluctuating cognitive impairment, Parkinson's disease-like symptoms, recurrent vivid visual hallucinations, and rapid eye movement sleep behavior disorder (RBD)¹. The pathological hallmarks of DLB are α -synuclein neuronal inclusions, and at least half of DLB patients in postmortem samples display variable degrees of Alzheimer's disease (AD)-related pathology^{2,3}. DLB accounts for 3.2% to 7.1% of dementia cases, ranking second only to AD⁴. However, due to its similarities with AD and Parkinson's disease (PD), DLB has a high clinical underdiagnosis and misdiagnosis rate⁵.

The etiology of DLB is exceedingly complex, involving both environmental and genetic factors. There is evidence that DLB exhibits family

clustering, with siblings of affected patients having a 2.3-fold increased risk of developing DLB, but little is known about the influence of genetic factors on DLB⁶. Based on clinical and pathological similarities, research has found genetic overlap between DLB, AD, and PD⁷⁻⁹. Previous scattered studies have identified *GBA*, *SNCA*, and *APOE* ϵ 4 allele variants as significant genetic risk factors for DLB¹⁰⁻¹³. In recent years, the first large-scale DLB genome-wide association study (GWAS) confirmed previously described gene associations, including *APOE*, *GBA*, and *SNCA*, and estimated the heritable component of DLB to be about 36%¹⁴. Subsequently, the largest DLB cohort study discovered five distinct genome-wide significant gene sites, including *GBA*, *BIN1*, *TMEM175*, *SNCA-AS1*, and *APOE*¹⁵. Genome-wide gene-aggregation tests implicated that the rare variants of *GBA* gene

¹Department of Neurology, Xiangya Hospital, Central South University, Changsha, China. ²National Clinical Research Center for Geriatric Disorders, Xiangya Hospital, Central South University, Changsha, China. ³Engineering Research Center of Hunan Province in Cognitive Impairment Disorders, Central South University, Changsha, China. ⁴Hunan International Scientific and Technological Cooperation Base of Neurodegenerative and Neurogenetic Diseases, Xiangya Hospital, Central South University, Changsha, China. ⁵Key Laboratory of Hunan Province in Neurodegenerative Disorders, Central South University, Changsha, China. ⁶Department of Geriatrics, Xiangya Hospital, Central South University, Changsha, China. ⁷Brain Research Center, Central South University, Changsha, Hunan, China. ⁸FuRong Laboratory, Central South University, Changsha, Hunan, China.

✉ e-mail: jiaobin@csu.edu.cn; shenlu@csu.edu.cn

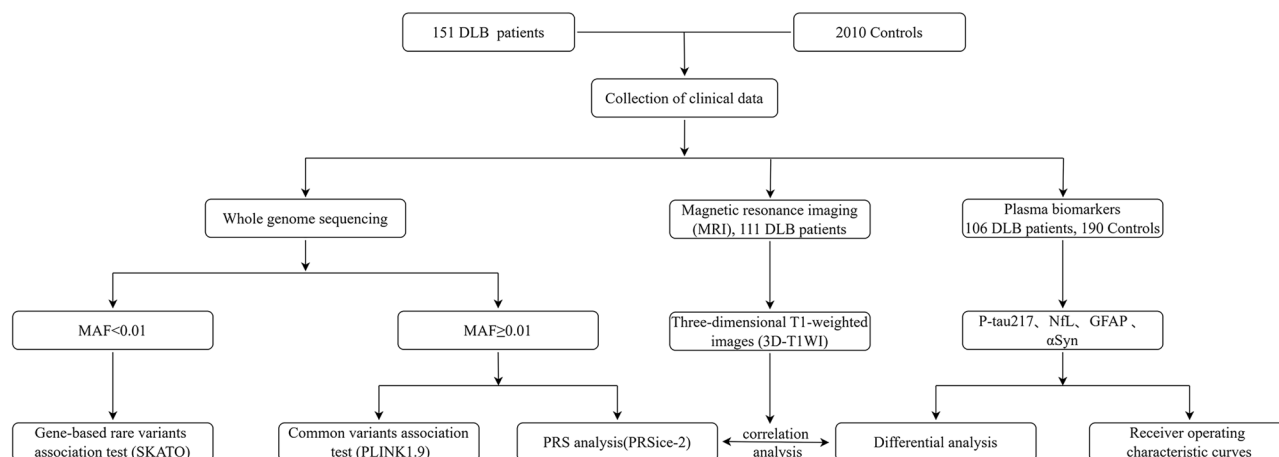


Fig. 1 | The flow chart in our study.

played a key role in the pathogenesis of DLB¹⁵. These findings underscore the strong hereditary component of DLB. Although genetics significantly contributes to the pathogenesis of DLB, current genetic research on DLB primarily focus on the Caucasian population, and investigations into the genetics of DLB in East Asian populations remain lacking.

Recently, changes of plasma biomarkers in neurodegenerative diseases have garnered attention^{16,17}. There are currently several studies investigating the alterations in plasma biomarkers among patients with DLB^{18,19}. Plasma p-tau181 and p-tau231 levels have been identified as helpful biomarkers for assessing cognitive decline in DLB patients¹⁹. Additionally, plasma NfL levels were elevated in high-risk prodromal DLB patients²⁰. Abnormal levels of GFAP have been detected at the stage of mild cognitive impairment with Lewy bodies (MCI-LB)²¹. However, most of these studies primarily focused on Caucasian population, and there is a lack of research on the relationship between plasma biomarkers and the genetic architecture of DLB. Therefore, comprehensive studies on plasma biomarkers and their association with genetic risk in a large cohort of Chinese DLB patients are necessary.

To sum up, the present study conducted whole genome sequencing (WGS) and plasma biomarker detection in DLB patients to identify candidate pathogenic variants and evaluate the diagnostic performance of plasma biomarkers among DLB patients in the Chinese population.

Results

Demographic and clinical characteristics

A total of 151 patients with DLB and 2010 healthy controls (HC) were included in this study (Fig.1). The average age of the DLB patients was 71.48 ± 9.18 years, while the average age at onset of DLB was 68.62 ± 9.36 years, and the average age of controls was 65.39 ± 8.41 years. There were significant differences in age between the two groups ($p < 0.001$). As expected, patients with DLB had lower Mini-Mental State Examination (MMSE) scores than the control group ($p < 0.001$). Additionally, 19.57% of DLB patients reported a family history of DLB, dementia, and/or Parkinson's syndrome. Demographic, clinical, and cognitive characteristics of participants are summarized in Table 1.

Common variant association analysis

Following quality control, a total of 7,897,572 common variants ($MAF \geq 0.01$) were involved in the association analysis. The Q-Q plot and genomic inflation factor ($\lambda_{1,000} = 1.048$) indicated good control of population stratification (Fig. 2A). Based on the Bonferroni-corrected p -value, GWAS identified a genome-wide-significant locus, the rs429358 locus of the *APOE* gene (effect allele (EA) = C, odds ratio [OR] = 3.071, 95% confidence interval [CI] = 2.214–4.261, effect allele frequency [EAF] in cases = 0.230, EAF in controls = 0.102, $p = 1.84E-11$) (Fig. 2B).

We investigated the impact of Caucasian DLB GWAS risk variants on DLB patients from Chinese population^{14,15}. Six of the eight known DLB risk

Table 1 | The demographic and clinical characteristics of the subjects

	DLB	HC	<i>p</i>
Number	151	2010	-
Gender (M/F)	82/69	931/1079	0.07
Age (mean \pm SD)	71.48 ± 9.18	65.39 ± 8.41	<0.001
MMSE (mean \pm SD)	14.69 ± 7.28	26.24 ± 2.73	<0.001
AAO (mean \pm SD)	68.62 ± 9.36	-	-
Duration of symptoms, years, median (IQR)	2 (1–4)	-	-
MOCA	8.09 ± 6.07	-	-
CDR	1.47 ± 0.73	-	-
Family History (%)	19.57%	-	-
Cognitive fluctuations (%)	70.20%	-	-
Visual hallucinations (%)	78.15%	-	-
RBD (%)	58.94%	-	-
Parkinsonism (%)	80.79%	-	-

DLB dementia with Lewy bodies, HC healthy controls, AAO age at onset, MMSE Mini-Mental State Examination, MOCA Montreal Cognitive Assessment, CDR Clinical Dementia Rating, RBD rapid eye movement sleep behavior disorder.

loci were retained in our cohort. Single variant association analysis revealed that three loci were nominally associated with DLB risk in our cohort ($p < 0.05$), including two loci in the *APOE* gene and one in the *BIN1* gene (Supplementary Table 1).

The genotype combination of rs429358 (T/C) and rs7412 (C/T) loci determines the three allelic variants of *APOE* ($\epsilon 2$, $\epsilon 3$ and $\epsilon 4$)²². The results revealed a substantial difference in *APOE* genotype distribution between 151 DLB patients and 2010 controls ($p < 0.001$). DLB patients had a considerably greater carrier rate of *APOE* $\epsilon 4$ (38.41%) compared to controls (17.41%) ($p = 4.08E-10$, Supplementary Fig. 1). We further conducted GWAS in participants carrying and not carrying the *APOE* $\epsilon 4$ allele, respectively, and no significant loci associated with DLB risk were identified in either group (Supplementary Fig. 2). This finding implies that the *APOE* $\epsilon 4$ (rs429358) locus plays a critical role in determining DLB risk.

Linear regression analysis of common variants in all patients with DLB was conducted using PLINK 1.9 to explore variants associated with age at onset (AAO) of DLB. This analysis revealed a suggestive association between the rs11987642 locus near the *DEFA5* gene and AAO of DLB in a clustered trend, although it was not statistically significant after Bonferroni

Fig. 2 | GWAS results. **A** The quantile-quantile (Q-Q) plot of common variant association results; **B** Manhattan plot of p values on the $-\log_{10}$ scale for common variant association analysis; **C** Manhattan plot of p values on the $-\log_{10}$ scale for common variant association analysis based on age at onset (AAO). **D** Manhattan plot of p values on the $-\log_{10}$ scale for gene-based association analysis. The horizontal red line represents the threshold of $p = 5 \times 10^{-8}$ for Bonferroni significance. The horizontal blue line represents the threshold of $p = 5.74 \times 10^{-5}$ (1/17423) for suggestive correlation of gene. GWAS genome-wide association study, DLB dementia with Lewy bodies, HC healthy controls.

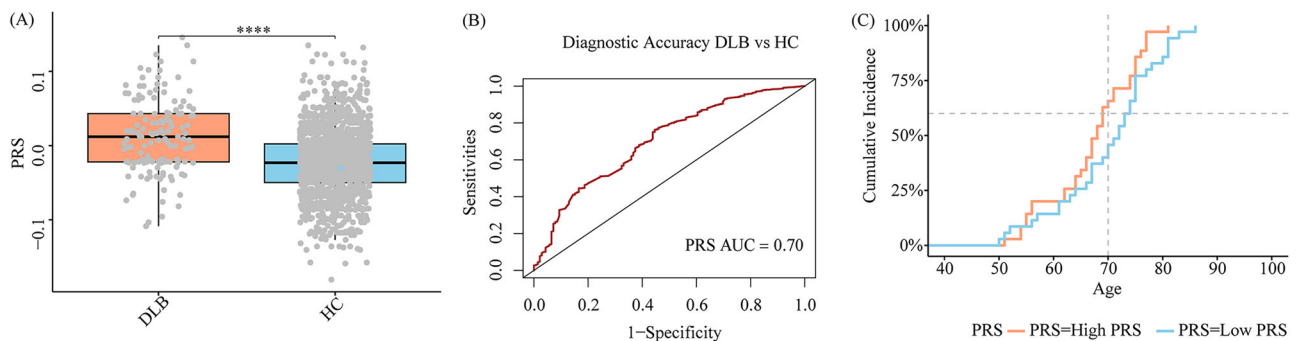
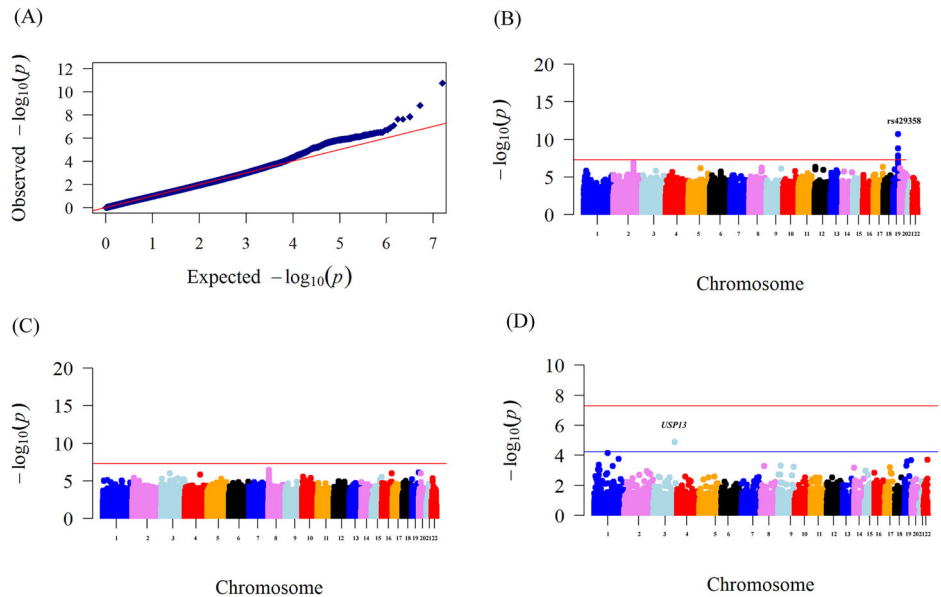


Fig. 3 | Discriminative and predictive performance of PRS in DLB patients. **A** PRS between DLB patients and controls. **B** The discriminative ability of PRS model for DLB. **C** The cumulative incidence rates of DLB in two genetic risk groups. PRS,

polygenic risk score; DLB, dementia with Lewy bodies, HC healthy controls, AUC area under the curve; ****, $p < 0.0001$.

correction ($p = 3.67 \times 10^{-7}$, Fig. 2C). Patients carrying the rs11987642 variant developed DLB at a considerably younger age (66.15 ± 9.85 years) compared to non-carriers (71.89 ± 7.32 years).

Gene-based rare variant association analysis

A total of 17,423 genes containing rare missense variants were included for analysis in the rare missense variant group (minor allele frequency (MAF) < 0.01 , missense variants). The results indicated a suggestive correlation between rare missense variants of *USP13* gene and DLB risk ($p = 1.31 \times 10^{-5}$, Fig. 2D). In the rare damaging variant group (MAF < 0.01 , ReVe > 0.7 or loss-of-function (LoF) variants), a total of 14,992 genes with damaging variants were included for analysis. However, none of these genes differed significantly between DLB patients and controls after multiple corrections.

Performance of polygenic risk score (PRS) in identifying and predicting DLB

The whole genome PRS of DLB was generated using PRSice-2, and the results showed that DLB patients had significantly higher PRS than the control group (PRS_{DLB} = 0.01 ($-0.02, 0.04$), PRS_{HC} = -0.02 ($-0.05, 0$), $p = 1.64 \times 10^{-15}$) (Fig. 3A). We assessed the ability of PRS to distinguish DLB from controls through receiver operating characteristic (ROC) analyses, which revealed an area under the curve (AUC) value of 0.70 (95% CI: 0.66–0.75) (Fig. 3B). All DLB patients were classified into quartiles based on

their PRS results. Utilizing the Cox proportional hazards model, we found that DLB patients in the highest quartile of PRS had an earlier AAO than those in the lowest quartile (AAO in the high PRS group: 67.06 ± 7.9 vs AAO in the low PRS group: 69.91 ± 9.24). Furthermore, the cumulative incidence rates in the high PRS group surpassed those in the low PRS group. For instance, the cumulative incidence rates of DLB in the high PRS group were higher than those in the low PRS group at the age of 70 s (60% vs 40%) (Fig. 3C).

Differential analysis and identification performance of plasma biomarkers

Plasma p-tau217, NfL, GFAP and α Syn levels were significantly elevated in DLB patients compared to controls ($p < 0.001$, Supplementary Table 2). Notably, plasma p-tau217 and GFAP levels were significantly increased in patients with mild DLB ($p < 0.0001$, Fig. 4A–D). ROC curves were employed to assess the ability of different plasma biomarkers in distinguishing DLB from controls. Plasma p-tau217 demonstrated the best discriminatory ability (AUC = 0.796), followed by GFAP (AUC = 0.781). The combination of plasma p-tau217, NfL, GFAP, α Syn, and PRS achieved an AUC of 0.927 for DLB diagnosis (Fig. 4E). Remarkably, this combination could distinguish mild DLB from controls with an AUC of 0.929 (Fig. 4F).

We further compared the levels of plasma biomarkers between DLB and AD patients, and significant differences in plasma p-tau217 and α Syn levels were observed between the two group ($p = 1.67 \times 10^{-3}$, $p = 1.79 \times 10^{-2}$,

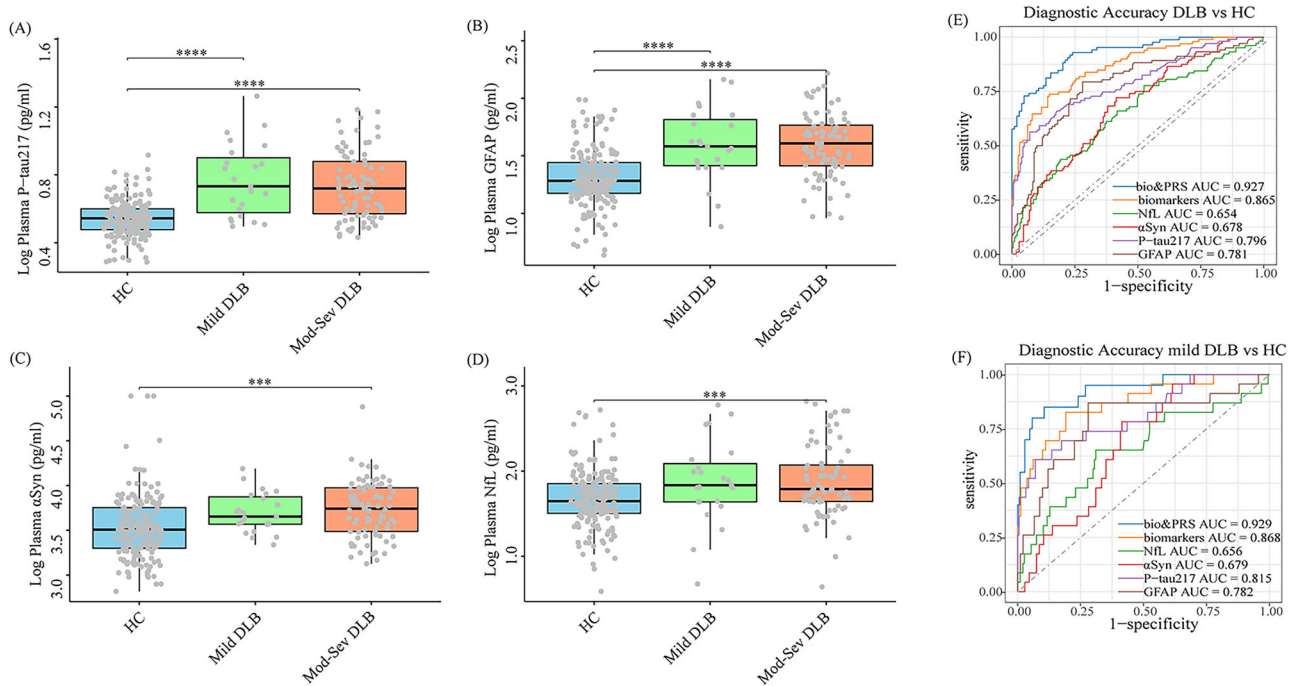


Fig. 4 | Performance of plasma biomarkers in differentiating and identifying DLB. A–D Comparisons of plasma biomarkers levels in healthy controls, mild DLB, and moderate-severe DLB. ANCOVA analysis was conducted for multiple comparisons with age and gender as covariates. The Bonferroni corrections were applied to p values of multiple comparisons. E ROC curves of each plasma biomarker and the combination with PRS for discriminating DLB from controls; F ROC curves of

each plasma biomarker and the combination with PRS for discriminating mild DLB from controls. DLB dementia with Lewy bodies, Mod-Sev DLB moderate-severe DLB, HC healthy controls, P-tau phosphorylated tau, NfL neurofilament light chain, GFAP glial fibrillary acidic protein, αSyn α-synuclein, ANCOVA analysis of covariance, ROC receiver-operating characteristic, AUC area under the curve, PRS polygenic risk score. *** p < 0.001; **** p < 0.0001.

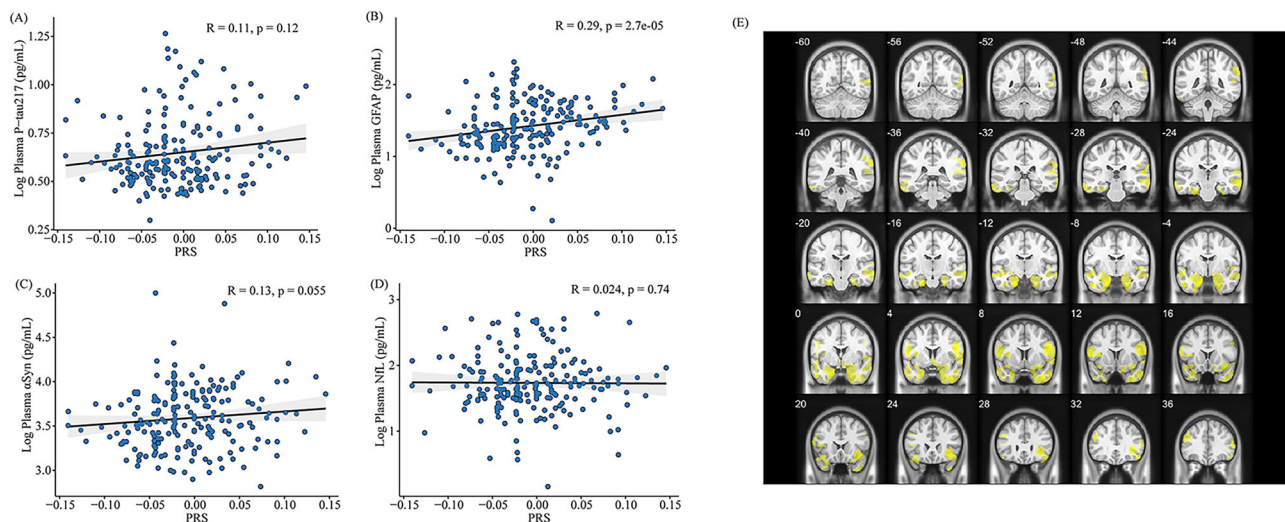


Fig. 5 | Correlations between PRS, plasma biomarkers and gray matter volume. A PRS and p-tau217; B PRS and GFAP; C PRS and αSyn; D PRS and NfL; E the voxel-based gray matter volume and plasma NfL levels in DLB patients. The yellow area in the plot represents the area negatively correlated with plasma NfL levels,

mainly concentrated in the bilateral temporal lobes. PRS polygenic risk score, P-tau phosphorylated tau, NfL neurofilament light chain, GFAP glial fibrillary acidic protein, αSyn α-synuclein, DLB dementia with Lewy bodies.

Supplementary Table 3). Furthermore, the combination of these four plasma biomarkers was able to discriminate DLB from AD with an AUC of 0.724 (Supplementary Fig. 3).

To explore the impact of the APOE ε4 allele on plasma biomarkers, we compared the plasma biomarker levels between DLB patients carrying APOE ε4 allele and those without APOE ε4 allele. However, no significant differences in plasma biomarker levels were observed between the two groups (Supplementary Fig. 4).

Association analysis of PRS with plasma biomarkers

Additionally, we analyzed the correlation of PRS with plasma p-tau217, NfL, GFAP, and αSyn levels in our cohort. The results revealed that PRSs of DLB were significantly correlated with plasma GFAP levels ($R = 0.29$, $p = 2.7E-05$) (Fig. 5A–D). Moreover, the correlation of plasma GFAP levels with PRS remained significant even after adjusting for age and gender using a general linear regression model ($\beta = 0.105$, adjusted $p = 4.66E-03$). The correlations between PRS and the other plasma biomarkers were not significant.

Association analysis between PRS, plasma biomarkers, and gray matter volume

We further investigated the correlation between PRS, plasma biomarkers, and gray matter volume. The findings showed that higher plasma NfL levels were prominently associated with greater atrophy of bilateral temporal lobes (Fig. 5E). No significant correlations were observed between the other plasma biomarkers, PRS, and brain atrophy.

Discussion

We conducted the first genetic research of DLB in an East Asian population and analyzed the association between genetic risk and plasma biomarkers in DLB patients for the first time. Our findings indicated that *APOE* $\epsilon 4$ allele significantly increased the risk of DLB, while the rare missense variant of *USP13* gene was first found to be suggestively associated with DLB risk in the Chinese population. PRSs of DLB patients were significantly associated with the risk of DLB, age at onset, as well as plasma GFAP levels. Furthermore, higher levels of plasma GFAP, α Syn, NfL, and p-tau217 were detected in DLB patients compared to controls, and these plasma biomarkers demonstrated a strong capacity to distinguish DLB from controls. Plasma GFAP levels could offer early screening and predict genetic risk for DLB. Additionally, higher plasma NfL level was significantly associated with greater atrophy of temporal lobes.

Several previous studies have demonstrated that *APOE* $\epsilon 4$ is the major genetic risk locus for DLB^{23,24}. The first large-scale GWAS of DLB based on Caucasian population found that the most significant association with DLB occurred at the *APOE* $\epsilon 4$ locus¹⁴. In our cohort, common variant association analysis revealed that the *APOE* rs429358 locus, which defines *APOE* $\epsilon 4$ ²⁵, was strongly associated with DLB risk, as it does in the Caucasian population. Approximately 38.41% of DLB patients carried the *APOE* $\epsilon 4$ locus in our cohort. The findings indicated that the *APOE* $\epsilon 4$ locus also acted as a strong risk factor for DLB in the East Asian population. Studies have shown that the *APOE* $\epsilon 4$ allele associated with DLB is mainly driven by a subset of concomitant AD pathology²⁶. A basic experiment demonstrated that *APOE* $\epsilon 4$ exacerbated α -synuclein seeding activity and neurotoxicity²⁷. Besides, three previously reported significant loci in Caucasian populations were nominally associated with DLB risk in our cohort, two in the *APOE* gene and one in the *BIN1* gene. This suggests that the effect of *APOE* gene on DLB pathogenesis is similar across different races. The inability of validating the remaining significant loci of Caucasian populations may be attributed to population differences and cohort size.

Since most risk single nucleotide polymorphisms exert small effects on disease susceptibility, PRS, which determine the genetic risk of disease by integrating the effects of multiple gene loci, have been widely used in the prediction of high-risk populations²⁸. Several studies on PRS of AD have identified an association between PRS of AD, age at onset, and cumulative incidence rates^{29,30}. However, there is still a lack of research on PRS in DLB patients. Our study showed that PRSs of DLB patients were significantly higher than controls, and the ROC analysis revealed an AUC value of 0.70, indicating that the PRS model had a fair ability to identify DLB patients³¹. Furthermore, we utilized the Cox proportional risk model to analyze the effect of PRS on the development of DLB and found that patients with higher PRS had a younger age at onset and higher cumulative incidence rates. Likewise, a large-scale GWAS analysis of DLB based on the Caucasian population discovered that DLB patients in the highest quintile of PRS exhibited more severe impairment than those in the lowest quintile¹⁴. These findings imply that genetic risk of DLB may influence both the cumulative incidence rates and the age at onset. The establishment of the PRS model helps clinicians judge DLB risk and provide assistance for early prevention and diagnosis for DLB. However, due to the limited number of DLB patients in our cohort, larger-scale GWAS involving DLB patients from the Chinese population will be needed to enhance the predictive capacity of the PRS model.

Gene-based analysis revealed a suggestive correlation between rare missense variant of *USP13* gene and DLB risk. The *USP13* gene encodes ubiquitin-specific protease-13 (USP13), a deubiquitinating enzyme

member of the cysteine-dependent protease superfamily³². Ubiquitination is a crucial mechanism for protein hydrolysis, while deubiquitination reduces protein degradation³³. Xiaoguang Liu's team discovered that one of the main reasons for the existence of Lewy bodies is the presence of USP13 molecule, which removes the "ubiquitin tags" from α -synuclein, making it difficult to be cleared by the human or animal body³⁴. The researchers then suppressed the formation of USP13 molecules in the PD mouse model, and the results revealed this could both eliminate Lewy bodies and prevent their re-accumulating³⁵. Our results confirm the association between *USP13* and DLB risk from a genetic perspective for the first time. Further validation of the role of *USP13* gene in modifying DLB risk will be important.

Plasma biomarkers have been extensively studied in AD, but less is known about their prognostic significance in DLB, particularly among the Chinese population. Our investigation revealed that plasma levels of p-tau217, NfL, GFAP, and α Syn were considerably higher in DLB patients compared to controls. Additionally, these plasma biomarkers offered good capacity in distinguishing DLB patients from controls or AD patients. Plasma p-tau217 exhibited the highest discriminatory ability for DLB, which was similar to prior plasma biomarker investigations of AD^{36,37}. Remarkably, plasma p-tau217 and GFAP levels were prominently increased in patients with mild DLB, indicating that plasma GFAP and p-tau217 levels had been significantly elevated in the mild stages of DLB. Comorbid AD neuropathology is common in DLB²⁰. Research indicated that plasma GFAP and p-tau181 could detect AD co-pathology in DLB patients, including A β and tau pathology^{21,38}. Besides, plasma p-tau217 had been shown to be an effective predictor of brain amyloid levels in preclinical and early AD³⁹. Therefore, the elevation of plasma p-tau217 and GFAP levels in DLB patients is mainly driven by AD co-pathology. A large longitudinal investigation of this cohort indicated that higher baseline GFAP, NfL, p-tau181, and p-tau231 levels were associated with poor MMSE scores in DLB patients, while plasma GFAP and NfL levels were associated with faster cognitive deterioration¹⁸. More importantly, recent research found that plasma GFAP levels were considerably elevated at the stage of MCI-LB, whereas abnormal plasma p-tau181 and NfL levels were observed at the latest stage of DLB²¹. In general, monitoring plasma GFAP and p-tau217 levels is particularly beneficial in the detection of early DLB.

This is the first study to investigate the relationship between the genetic risk of DLB and plasma biomarkers. We discovered that PRSs of DLB were significantly positively associated with plasma GFAP levels, implying that the genetic architecture could predict the physiologic and pathological alterations of DLB to some extent. Based on plasma biomarker difference analysis and correlation analysis with PRS, we found that plasma GFAP level was elevated in mild DLB and was associated with PRSs of DLB. A recent study on the DLB continuum found that elevated GFAP level was observed in the prodromal phase of MCI-LB in association with increased amyloid burden, demonstrating that plasma GFAP level could be employed to detect amyloid-related pathology in the prodromal stage of DLB²¹. These findings suggested that detecting plasma GFAP levels could offer early screening and predict genetic risk for DLB.

Strong correlations were observed between plasma NfL levels and gray matter volume of the temporal lobe in our study. NfL is released into cerebrospinal fluid and blood following axonal damage, indicating neurodegenerative processes⁴⁰. A longitudinal study observed that baseline plasma NfL levels could predict cognitive decline in DLB patients after 2-year follow-up⁴¹. Another large prospective study found that higher baseline NfL levels in DLB patients indicated faster cognitive decline and plasma NfL possibly acted as a monitoring biomarker for cognitive symptoms in DLB¹⁷. Our findings further supported that plasma NfL levels could be used to monitor the progression of DLB disease.

This study had several limitations. First, the sample size of the DLB group was relatively small, which limited our capacity to detect rare genetic variants. Second, due to the overlap between the clinical phenotype of DLB and other diseases, the clinical diagnosis of DLB may be challenging. To reduce the possibility of misdiagnosis, the vast majority of DLB patients in our cohort met the diagnostic criteria for clinically probable DLB¹. Third,

our study did not correct the effect of AD co-pathology on the genetic association and plasma biomarker analysis related to DLB, and we will explore this impact in our future study.

In summary, our study filled the gap in the genetics of DLB in East Asia and highlighted the diagnostic efficacy of plasma biomarkers and PRS for DLB. We found that the *APOE* $\epsilon 4$ allele greatly increased the risk of DLB, and rare missense variants of *USP13* gene were first observed to be suggestively associated with DLB risk. The PRS model could predict the risk of DLB, the age at onset, as well as the biological changes of DLB to some extent.

Methods

Participants

A total of 151 DLB patients and 2010 healthy controls were enrolled in this study. The DLB patients were from the Department of Neurology, Xiangya Hospital, Central South University. The DLB patients met the diagnostic criteria for DLB by the International DLB Consortium in 2017¹. Besides, DLB patients were classified into mild DLB (CDR = 0.5–1) and moderate-severe DLB (CDR = 2–3) based on the CDR scores⁴². Controls were recruited from a community-based cohort in Hunan Province. There were no neurological disorders in the control group, and objective examination indicated normal cognition. The study followed the Declaration of Helsinki and was approved by the Ethics Committee of Xiangya Hospital of Central South University. Each participant or guardian provided their written informed consent.

Gene sequencing

Genomic DNA was extracted from peripheral blood leukocytes of subjects using the phenol chloroform method⁴³. All DNA samples were standardized at 100 ng/ μ L. Genomic DNA was fragmented, end repaired, ligated, and amplified by polymerase chain reaction (PCR) to establish a DNA library. After quality control of the library, sequencing was performed using the BGI-seq 500 platform. The average sequencing depth of this cohort is 39.29 \times , and the average coverage is 95.37%. The reads of low-quality fastq data were filtered out through FastQC, and the raw sequencing data was aligned with the human reference genome (GRCh38) using BWA software⁴⁴. Duplicate sequences were removed by Picard. GATK and ANNOVAR software were used to call variants and annotation variants, respectively^{45,46}.

Genetic variant analysis

Variants with genotype quality <30, Hardy Weinberg equilibrium $P < 1 \times 10^{-6}$, and genotyping rate <95% were filtered out using PLINK 1.9. Besides, allelic balance out of 25%/75% ratio of referent and alternate allele reads in the heterozygote, and allelic balance out of 95% ratio of in the homozygote were filtered out. Samples with gender inconsistency (gender inconsistency between self-reported gender and genotypic gender), kinship (PI-HAT statistic > 0.125)⁴⁷, high or low heterozygosity were excluded. The quality-controlled variants were classified as common variants (MAF \geq 0.01) and rare variants (MAF < 0.01) based on their MAF in this cohort. Our study defined the damaging variants as damaging missense variants (ReVe > 0.7) or LoF variants, which comprise variants resulting in stop, frameshift, or splice-site disruption⁴⁸.

We calculated the relevant genetic principal components using PLINK 1.9. Then, twstats of EIGENSTRAT was utilized to perform tests of significance on each principal component and principal components with $p < 0.05$ were included to control population stratification⁴⁹. We employed Q-Q plots and genomic inflation factors (λ) to assess for residual effects of population stratification that could not be fully controlled by principal component analysis and covariates in the regression model. The equivalent inflation factor for a study of 1000 cases and 1000 controls ($\lambda_{1,000}$) was rescaled using the following formula: $\lambda_{1,000} = 1 + 500 \times (\lambda - 1) \times (1/N_{cases} + 1/N_{controls})^{50,51}$. PLINK 1.9 was used to conduct logistic regression association analysis based on common variants, with covariates including age, gender, and the first eleven principal components taken into account.

Sequential Kernel Association Test-Optimal (SKAT-O) tests were used to perform gene-based association test by aggregating rare variants, and we included gender, age, and the first eleven principal components as covariates. Rare variants were divided into two categories: rare damaging variants (MAF < 0.01, LoF or ReVe > 0.7) and rare missense variants (MAF < 0.01, missense variants). Finally, linear regression analyses were performed in DLB patients using PLINK 1.9 to detect common variants associated with AAO of DLB, with gender and the first four principal components included as covariates. Statistical significance was defined as p -values* $n < 0.05$ (n being the number of variations or genes).

Magnetic resonance imaging (MRI)

A total of 111 DLB patients in this cohort underwent MRI examination at our center, of which 35 DLB patients completed the three-dimensional T1-weighted imaging (3D-T1WI) examination. MRI was conducted on a 3 T Siemens Prisma MRI scanner (Prisma, Siemens, Germany) with a 64-channel head/neck coil. The 3D-T1WI were acquired using a magnetization prepared rapid acquisition gradient echo (MPRAGE) sequence with the following parameters: Sagittal, 176 slices, slice thickness (ST) = 1 mm, repetition time (TR) = 2300 ms, echo time (TE) = 2.98 ms, inversion time (TI) = 900 ms, data matrix = 248 \times 256, field of view (FOV) = 248 \times 256 mm², and flip angle (FA) = 9°. Cortical thickness and gray matter volume were estimated using the CAT12 toolbox (<http://dbm.neuro.uni-jena.de/cat/>), which was implemented in SPM12 and run in MATLAB. Images were examined for internal quality assurance using CAT12-recommended values and indications. All images were segmented into gray matter, white matter, and cerebrospinal fluid, and normalized using the DARTEL algorithm. We smoothed the images with an isotropic Gaussian kernel of 10 mm full width half maximum.

Detection of plasma biomarkers

Among the WGS cohort, a subgroup of 106 DLB patients and 190 healthy controls underwent plasma biomarkers testing. In addition, 106 AD patients⁵² completed the same plasma biomarkers testing for comparison. Participants' venous blood was collected in EDTA tubes and centrifuged at 3000 rpm for 15 minutes at 4 °C within two hours of collection. Plasma samples were stored at -80 °C and not freeze-thawed before using in the experiment. Quantitative analysis of p-tau217, NfL, GFAP, and α -synuclein was performed on a fully automated single-molecule immune detection (SMID) machine (AST ScLite; AstraBio, Suzhou, China). The detailed working process of SMID in Astra System is shown in the Supplementary materials. We employed p-tau217 (R64100), NfL (R64040), GFAP (R64060), and α -synuclein (R64070) assay kits (AstraBio) for detection, respectively. The testing physician was unaware of the grouping of participants.

Statistical analysis

Demographic and clinical characteristics were summarized as means and standard deviations (SD), median and IQR, or percentages. Continuous variables with a normal distribution were analyzed for differences using the t-tests or analysis of covariance (ANCOVA), otherwise the Mann-Whitney U tests or Kruskal-Wallis tests were applied. Differences in categorical variables were evaluated using the chi-square test or Fisher's exact test.

The PRS was generated using PRSice-2⁵³. We incorporated genes identified in the latest published DLB GWAS to create a PRS model^{13,14}. All DLB patients were divided into four groups based on their PRS quartiles. The Cox proportional hazard model was used to investigate the association between PRS scores, age at onset, and the cumulative incidence rate of DLB. Plasma biomarker values were log-transformed with base 10 to approximate a normal distribution, and ANCOVA analysis was conducted for multiple comparisons with age and gender as covariates. To assess the efficacy of PRS and plasma biomarkers in discriminating DLB patients from controls or AD patients, the ROC analyses were performed to calculate the AUC. The associations between PRS and plasma biomarkers were evaluated using Spearman correlation tests and general linear regression models adjusted by

age and gender. To analyze the relationship between voxel-based gray matter volume, PRS scores, and plasma biomarker levels, the brain model was segmented and smoothed with CAT12. The MRI data were smoothed with an $8 \times 8 \times 8$ mm FWHM Gaussian kernel. Correlations were evaluated by general linear model analysis using SPM12, adjusted by gender, age, and the total intracranial volume. Statistical analysis was performed using R version 4.4.1. Statistical significance was deemed at $p < 0.05$ (two-tailed).

Data availability

The data are available on reasonable request to the corresponding author.

Code availability

The related codes and scripts for the study will be made available upon reasonable request to the corresponding author.

Received: 26 November 2024; Accepted: 2 May 2025;

Published online: 15 May 2025

References

- McKeith, I. G. et al. Diagnosis and management of dementia with Lewy bodies: fourth consensus report of the DLB Consortium. *Neurology* **89**, 88–100 (2017).
- Walker, Z., Possin, K. L., Boeve, B. F. & Aarsland, D. Lewy body dementias. *Lancet* **386**, 1683–1697 (2015).
- Irwin, D. J. et al. Neuropathological and genetic correlates of survival and dementia onset in synucleinopathies: a retrospective analysis. *Lancet Neurol.* **16**, 55–65 (2017).
- Hogan, D. B. et al. The prevalence and incidence of dementia with lewy bodies: a systematic review. *Can. J. Neurol. Sci.* **43**, S83–S95 (2016).
- Sanford, A. M. Lewy body dementia. *Clin. Geriatr. Med.* **34**, 603–615 (2018).
- Nervi, A. et al. Familial aggregation of dementia with Lewy bodies. *Arch. Neurol.* **68**, 90–93 (2011).
- Meeus, B. et al. DLB and PDD: a role for mutations in dementia and Parkinson disease genes?. *Neurobiol. Aging* **33**, 629.e625–629.e618 (2012).
- Arnautoglou, N. A., O'Brien, J. T. & Underwood, B. R. Dementia with Lewy bodies - from scientific knowledge to clinical insights. *Nat. Rev. Neurol.* **15**, 103–112 (2019).
- van der Lee, S. J. et al. Genetics contributes to concomitant pathology and clinical presentation in dementia with lewy bodies. *J. Alzheimers Dis.* **83**, 269–279 (2021).
- Keogh, M. J. et al. Exome sequencing in dementia with Lewy bodies. *Transl. Psychiatry* **6**, e728 (2016).
- Orme, T. et al. Analysis of neurodegenerative disease-causing genes in dementia with Lewy bodies. *Acta Neuropathol. Commun.* **8**, 5 (2020).
- Vergouw, L. J. M. et al. An update on the genetics of dementia with Lewy bodies. *Parkinsonism Relat. Disord.* **43**, 1–8 (2017).
- Lerche, S. et al. Dementia with lewy bodies: GBA1 mutations are associated with cerebrospinal fluid alpha-synuclein profile. *Mov. Disord.* **34**, 1069–1073 (2019).
- Guerreiro, R. et al. Investigating the genetic architecture of dementia with Lewy bodies: a two-stage genome-wide association study. *Lancet Neurol.* **17**, 64–74 (2018).
- Chia, R. et al. Genome sequencing analysis identifies new loci associated with Lewy body dementia and provides insights into its genetic architecture. *Nat. Genet.* **53**, 294–303 (2021).
- Balogun, W. G., Zetterberg, H., Blennow, K. & Karikari, T. K. Plasma biomarkers for neurodegenerative disorders: ready for prime time?. *Curr. Opin. Psychiatry* **36**, 112–118 (2023).
- Cousins, K. A. Q. et al. Pathologic and cognitive correlates of plasma biomarkers in neurodegenerative disease. *Alzheimers Dement.* **20**, 3889–3905 (2024).
- Bolsewig, K. et al. Association of plasma amyloid, P-Tau, GFAP, and NfL With CSF, clinical, and cognitive features in patients with dementia with lewy bodies. *Neurology* **102**, e209418 (2024).
- Gonzalez, M. C. et al. Association of Plasma p-tau181 and p-tau231 concentrations with cognitive decline in patients with probable dementia with lewy bodies. *JAMA Neurol.* **79**, 32–37 (2022).
- Hiraga, K. et al. Plasma biomarkers of neurodegeneration in patients and high risk subjects with Lewy body disease. *NPJ Parkinsons Dis.* **10**, 135 (2024).
- Diaz-Galvan, P. et al. Plasma biomarkers of Alzheimer's disease in the continuum of dementia with Lewy bodies. *Alzheimers Dement.* **20**, 2485–2496 (2024).
- Raulin, A. C. et al. ApoE in Alzheimer's disease: pathophysiology and therapeutic strategies. *Mol. Neurodegener.* **17**, 72 (2022).
- Tsuang, D. et al. APOE $\epsilon 4$ increases risk for dementia in pure synucleinopathies. *JAMA Neurol.* **70**, 223–228 (2013).
- Bras, J. et al. Genetic analysis implicates APOE, SNCA and suggests lysosomal dysfunction in the etiology of dementia with Lewy bodies. *Hum. Mol. Genet.* **23**, 6139–6146 (2014).
- Kulminski, A. M. et al. Associations of the APOE $\epsilon 2$ and $\epsilon 4$ alleles and polygenic profiles comprising APOE-TOMM40-APOC1 variants with Alzheimer's disease biomarkers. *Aging* **14**, 9782–9804 (2022).
- Peuralinna, T. et al. Genome-wide association study of neocortical Lewy-related pathology. *Ann. Clin. Transl. Neurol.* **2**, 920–931 (2015).
- Jin, Y. et al. APOE4 exacerbates α -synuclein seeding activity and contributes to neurotoxicity in Alzheimer's disease with Lewy body pathology. *Acta Neuropathol.* **143**, 641–662 (2022).
- Khera, A. V. et al. Genome-wide polygenic scores for common diseases identify individuals with risk equivalent to monogenic mutations. *Nat. Genet.* **50**, 1219–1224 (2018).
- Li, W. W. et al. Association of polygenic risk score with age at onset and cerebrospinal fluid biomarkers of alzheimer's disease in a chinese cohort. *Neurosci. Bull.* **36**, 696–704 (2020).
- Jiao, B. et al. Associations of risk genes with onset age and plasma biomarkers of Alzheimer's disease: a large case-control study in mainland China. *Neuropsychopharmacology* **47**, 1121–1127 (2022).
- Nahm, F. S. Receiver operating characteristic curve: overview and practical use for clinicians. *Korean J. Anesthesiol.* **75**, 25–36 (2022).
- Reyes-Turcu, F. E. et al. The ubiquitin binding domain ZnF UBP recognizes the C-terminal diglycine motif of unanchored ubiquitin. *Cell* **124**, 1197–1208 (2006).
- Lonskaya, I., Desforges, N. M., Hebron, M. L. & Moussa, C. E. Ubiquitination increases parkin activity to promote autophagic α -synuclein clearance. *PLoS ONE* **8**, e83914 (2013).
- Liu, X., Hebron, M., Shi, W., Lonskaya, I. & Moussa, C. E. Ubiquitin specific protease-13 independently regulates parkin ubiquitination and alpha-synuclein clearance in alpha-synucleinopathies. *Hum. Mol. Genet.* **28**, 548–560 (2019).
- Liu, X. et al. Inhibition of Ubiquitin-Specific Protease-13 improves behavioral performance in Alpha-Synuclein expressing mice. *Int. J. Mol. Sci.* **23**, <https://doi.org/10.3390/ijms23158131> (2022).
- Therriault, J. et al. Equivalence of plasma p-tau217 with cerebrospinal fluid in the diagnosis of Alzheimer's disease. *Alzheimers Dement.* **19**, 4967–4977 (2023).
- Palmqvist, S. et al. Discriminative accuracy of plasma Phospho-tau217 for Alzheimer disease vs other neurodegenerative disorders. *Jama* **324**, 772–781 (2020).
- Vrillon, A. et al. Plasma biomarkers of amyloid, tau, axonal, and neuroinflammation pathologies in dementia with Lewy bodies. *Alzheimers Res. Ther.* **16**, 146 (2024).
- Devanarayan, V. et al. Plasma pTau217 predicts continuous brain amyloid levels in preclinical and early Alzheimer's disease. *Alzheimers Dement.* **20**, 5617–5628 (2024).

40. Jung, Y. & Damoiseaux, J. S. The potential of blood neurofilament light as a marker of neurodegeneration for Alzheimer's disease. *Brain* **147**, 12–25 (2024).
41. Pilotto, A. et al. Plasma Neurofilament Light Chain Predicts Cognitive Progression in Prodromal and Clinical Dementia with Lewy Bodies. *J. Alzheimers Dis.* **82**, 913–919 (2021).
42. Hughes, C. P., Berg, L., Danziger, W. L., Coben, L. A. & Martin, R. L. A new clinical scale for the staging of dementia. *Br. J. Psychiatry* **140**, 566–572 (1982).
43. Di Pietro, F., Ortenzi, F., Tilio, M., Concetti, F. & Napolioni, V. Genomic DNA extraction from whole blood stored from 15- to 30-years at -20 °C by rapid phenol-chloroform protocol: a useful tool for genetic epidemiology studies. *Mol. Cell Probes* **25**, 44–48 (2011).
44. Li, H. & Durbin, R. Fast and accurate long-read alignment with Burrows-Wheeler transform. *Bioinformatics* **26**, 589–595 (2010).
45. McKenna, A. et al. The Genome Analysis Toolkit: a MapReduce framework for analyzing next-generation DNA sequencing data. *Genome Res.* **20**, 1297–1303 (2010).
46. Wang, K., Li, M. & Hakonarson, H. ANNOVAR: functional annotation of genetic variants from high-throughput sequencing data. *Nucleic Acids Res.* **38**, e164 (2010).
47. Chia, R. et al. Genome sequence analyses identify novel risk loci for multiple system atrophy. *Neuron* **112**, 2142–2156.e2145 (2024).
48. Li, J. et al. Performance evaluation of pathogenicity-computation methods for missense variants. *Nucleic Acids Res.* **46**, 7793–7804 (2018).
49. Patterson, N., Price, A. L. & Reich, D. Population structure and eigenanalysis. *PLoS Genet* **2**, e190 (2006).
50. Cai, Q. et al. Genome-wide association analysis in East Asians identifies breast cancer susceptibility loci at 1q32.1, 5q14.3 and 15q26.1. *Nat. Genet.* **46**, 886–890 (2014).
51. Freedman, M. L. et al. Assessing the impact of population stratification on genetic association studies. *Nat. Genet.* **36**, 388–393 (2004).
52. McKhann, G. M. et al. The diagnosis of dementia due to Alzheimer's disease: recommendations from the National Institute on Aging-Alzheimer's Association workgroups on diagnostic guidelines for Alzheimer's disease. *Alzheimers Dement.* **7**, 263–269 (2011).
53. Choi, S. W. & O'Reilly, P. F. PRSice-2: Polygenic Risk Score software for biobank-scale data. *Gigascience* **8**, <https://doi.org/10.1093/gigascience/giz082> (2019).

Acknowledgements

We sincerely thank all of the participants for their commitment in participating and donating blood samples for this study. This study was supported by the STI2030-Major Projects (2021ZD0201803), the National Natural Science Foundation of China (U22A20300, 82071216, 82371434), the Science and Technology Major Project of Hunan Province (2021SK1020), Outstanding Youth Fund of Hunan Provincial Natural Science Foundation (2024JJ2097), Hunan Health Commission (20232460),

Hunan Innovative Province Construction Project (2021SK1010), Hunan Provincial Natural Science Foundation of China (2023JJ40792), the Grant of National Clinical Research Center for Geriatric Disorders, Xiangya Hospital (2022LNJJ16), and Postdoctoral Fellowship Program of CPSF (GZC20233185).

Author contributions

L.S. and B.J. had full access to all of the data in the study and took responsibility for the integrity of the data and the accuracy of the data analysis. L.S., B.J., J.C.L., B.S.T., and S.L.L. designed the study. Participant recruitment and data collection: X. L.H., X.W.X., L.W., Z.J.L., Q.X., J.D., Q.J.Y., Y.Z., Y.L.L., T.Y.X., Y.F.Z., X.X.L., J.F.G., J.L.W., and X.X.Y. X.L.H. analyzed the data and drafted the manuscript. X.L.H., S.L.L., B.S.T., J.C.L., B.J. and L.S. made critical revision of the manuscript. L.S. and B.J. supervised the completion of this study.

Competing interests

The authors declare no competing interests.

Additional information

Supplementary information The online version contains supplementary material available at <https://doi.org/10.1038/s41531-025-00988-z>.

Correspondence and requests for materials should be addressed to Bin Jiao or Lu Shen.

Reprints and permissions information is available at <http://www.nature.com/reprints>

Publisher's note Springer Nature remains neutral with regard to jurisdictional claims in published maps and institutional affiliations.

Open Access This article is licensed under a Creative Commons Attribution-NonCommercial-NoDerivatives 4.0 International License, which permits any non-commercial use, sharing, distribution and reproduction in any medium or format, as long as you give appropriate credit to the original author(s) and the source, provide a link to the Creative Commons licence, and indicate if you modified the licensed material. You do not have permission under this licence to share adapted material derived from this article or parts of it. The images or other third party material in this article are included in the article's Creative Commons licence, unless indicated otherwise in a credit line to the material. If material is not included in the article's Creative Commons licence and your intended use is not permitted by statutory regulation or exceeds the permitted use, you will need to obtain permission directly from the copyright holder. To view a copy of this licence, visit <http://creativecommons.org/licenses/by-nc-nd/4.0/>.

© The Author(s) 2025